УДК 528.8.044.2 DOI: https://doi.org/10.24028/gj.v45i1.275180

Application of Sentinel-1 radar interferometric images for the monitoring of vertical displacements of the earth's surface affected by non-tidal atmospheric loading

K.R. Tretyak[1], *D.V. Kukhtar*[2], *2023*

[1]Lviv Polytechnic National University, Lviv, Ukraine
[2]Ivano-Frankivsk National Technical University of Oil and Gas, Ivano-Frankivsk, Ukraine
Received 4 July 2022

The vertical movements of the Earth's surface affected by non-tidal atmospheric loading (NTAL) are analyzed using satellite radar interferometry data. A clear relationship between deformation maps data derived from radar interferometry data and the GNSS time series of permanent stations has been established. The object of the study was the areas around the GNSS stations BYCH (Buchach), GORD (Horodok), CRNT (Chernivtsi). The input data were four pairs of radar interferometric images for the specified areas.Radar satellite images were obtained from the Sentinel-1A spacecraft. Data type — SLC (Single Look Complex) with vertical polarization. Acquisition mode — wideband interferometric IW (Interferometric Wide Swath). Data were processed using SNAP (Sentinel Application Platform) software. The processing yileded maps of vertical displacement of the specified territories where the earth's surface displacement caused by influence of non-tidal atmospheric loading had taken place. The values obtained on the basis of vertical displacement maps have a high agreement with the results of time series of changes in the altitude position of permanent GNSS stations. The results obtained in the article are of both scientific and practical importance for studying the impact of non-tidal atmospheric loading in large areas. The practical significance is in improving the accuracy of terrestrial geodetic measurements' processing, in particular high-precision levelling. The research data allow to make corrections of the results of levelling for short-period displacements affected by the influence of non-tidal atmospheric loading (NTAL).

Key words: GNSS time series, vertical displacement, non-tidal atmospheric loading, radar interferometry, Sentinel-1.

Introduction. It is known that environmental factors influence the results of the GNSS time series. One of such factors is Non-Tidal Loading [Gobron et al., 2021]. The result of the non-tidal load influence is the displacement of the earth's surface. Thus spatial position of objects changes including permanent stations. Taking into account this factor, it reduces by 20 % on average the error in the analysis of vertical motions of the earth surface [Mémin et al., 2020].

The components of non-tidal load are the Non-Tidal Atmospheric Loading and the Non-Tidal Ocean Loading. The first factor is determinedon the basis of the ground atmospheric pressure. The information about the change of vertical position of earth surface is processed by GFZ Geo Research Center in Potsdam (Geo Forschungs Zentrum) (http://esmdata.gfz-potsdam.de:8080/repository/) based on the data of medium-term weather forecasts ECMWF (European Center for Medium-Range Weather Forecasts).The calculations of the earth surface displacement under the action of NTAL can be loaded from the International Mass Loading Service [Petrov, 2015] and Vienna Mapping Functions Open Access Data [VMF]. Vertical displacements

of time series of these three models for the territory of the western part of Ukraine are almost identical with the average deviations within the limits of a 1 mm and the maximum up to 3 mm.

The second factor is formed through the redistribution of the masses on the ocean floor and the change of pressure in the river network of the region [Klos et al., 2021]; the model of MPIOM (Max Planck Institute Ocean Model) is used for calculations [Jungclaus et al., 2013].

The vertical displacement of GNSS stations in Europe was recorded on the territory of Europe at the end of December 2019. For a short time (5—10 days) (Fig. 1), subsidence reached 30 mm [Brusak, Tretyak, 2020].

This displacement was fixed on the territory of Ukraine by the permanent stations of the GNSS network «Geoterrace». The value of subsidence of GNSS stations (Fig. 2) reached 12—27 mm within 5—6 days [Tretyak et al., 2021]. For the territory of Ukraine, the maximum altitude displacement occurred on 23—30 December, 2019 (the 357th—364th days of the year).

According to these studies, a precise interrelation was established between the change in the altitude position of GNSS stations and vertical displacements caused by non-tidal atmospheric load calculated by GFZ, which was 20 mm for the research area (http://esmdata.gfzpotsdam.de: 8080/repository/).

It is necessary to note that the spatial distribution of GNSS stations' subsidence allows differentiating the research area into two blocks (see Fig. 2). The central unit is characterized by an average subsidence of 12 mm GNSS stations, and the second unit, which surrounds the central unit, experienced an average subsidence of 19 mm. The difference in the nature of vertical displacements is partly explained by the heterogeneity of the geological structure of the territory. Accordingly, the actual act of the displacements caused by NTAL may differ significantly from the data calculated according to the data of atmospheric meteorological parameters.

Detailing the distribution of vertical displacements of the territory under NTAL influence is not only of scientific interest, but has practical significance. These inhomogeneous movements of the earth surface should be taken into account while calculating the stability of large engineering structures, in particular whilst designing HPP, PSP, NPP,

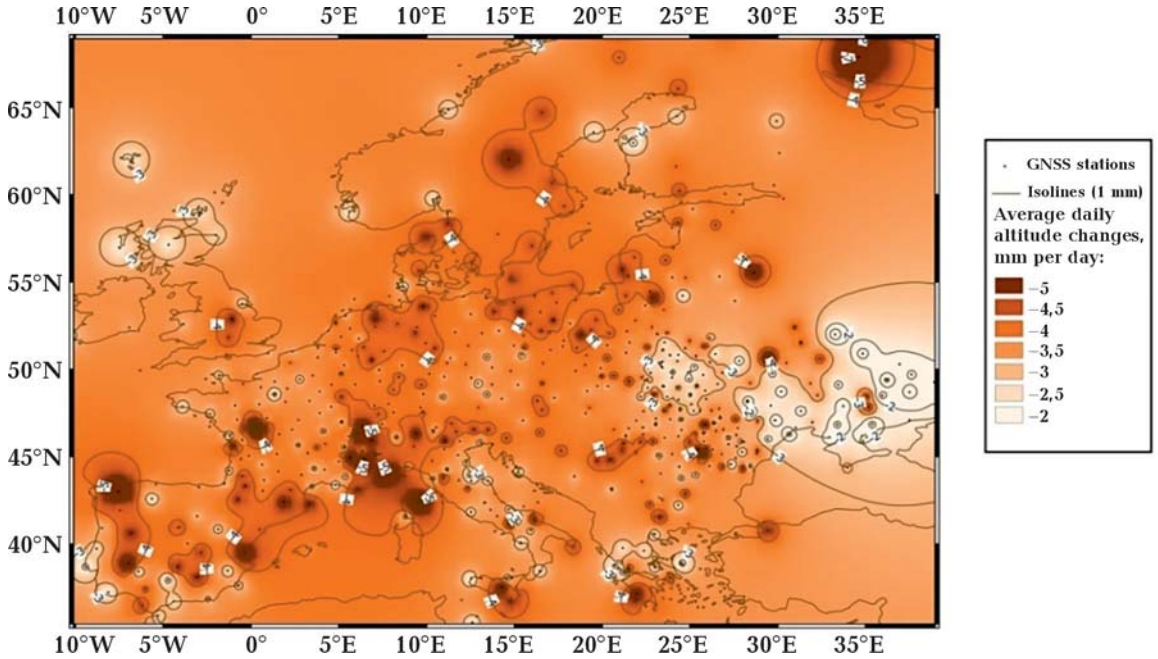

Fig. 1. The average daily subsidence of the earth surface in Europe from 20.12 to 30.12.2019, according to GNSS stations [Brusak, Tretyak, 2020].

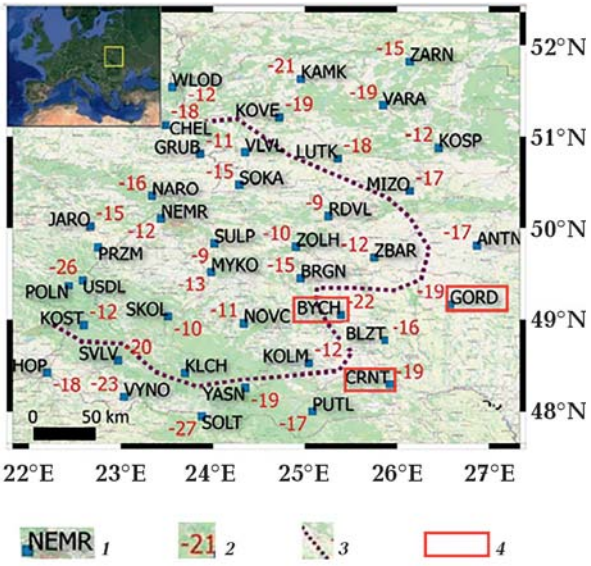

Fig. 2. Dynamics of the vertical displacement of GNSS station of Geoterrace networkin December 2019 [Brusak, Tretyak, 2021]: *1* — GNSS station; *2* — vertical displacement, mm; *3* — line dividing GNSS stations into 2 groups; *4* — GNSS stations are selected for research.

bridges, overpasses. Besides this, while doing the geodetic work it is necessary to make appropriate residuals in the heights and coordinates of the benchmarks for changing their position under the influence of NTAL, which can significantly increase the accuracy of measurements and their reliability.

The basic method of geodetic monitoring for vertical and horizontal movements of the earth surface is the analysis of data from permanent GNSS stations. The drawback of this method is that the results of displacements are obtained at particular points on the earth surface. Currently, networks of permanent GNSS stations are designed so that the stations are 70—80 km apart. Accordingly, analyzing local movements of the earth surface for the construction of large engineering structures in such networks is impossible.

In recent years, remote radar sensing data have become widely used in addition to the GNSS measurements on permanent networks. The use of radar data with Synthetic Aperture Radar (SAR) makes it possible to develop almost continuous maps of displacements of the earth surface with millimeter accuracy. The vertical displacement mapsare created on the basis of Differential SAR Interferometry (DInSAR). Radar interferometry data are processedby several methods. The most common approaches include the Small Baseline Subset (SBAS) [Li et al., 2022] and the Persistent Scatterer Interferometry (PSI) method [Crosetto et al., 2016].

This method is widely used for monitoring earthquakes and volcanic activity [Lu et al., 2010; Schaefer et al., 2015], landslide areas [Tzouvaras et al., 2020], areas where minerals are mined [Sheng et al., 2009; Stankevich et al., 2019; Dorosh, Gera, 2020], active geodynamic regions [Uglitskih et al., 2020], glaciological processes [Amitrano et al., 2019; Gómez et al., 2020]. The list of applications is much longer and concerns the monitoring of the environment and safety issues.

In this research, an attempt was made to use satellite radar interferometry data for spatial information about the distribution of vertical displacements of the earth surface caused by NTAL. Adjacent areas to three GNSS stations of the Geoterrace network were selected for experimental studies: BYCH (Buchach), GORD (Horodok) and CRNT (Chernivtsi), located in Ternopil, Khmelnytskyi and Chernivtsi regions, respectively (see Fig. 2). The studies cover the period of active vertical displacement of GNSS stations and the manifestation of NTAL from 16.12.2019 to 01.01.2020.

The purpose of the research is to analyze the possibilities of determining, estimating and mapping the spatial distribution of vertical movements of the Earth's surface, under the influence of anomalous non-tidal atmospheric loads, according to satellite radar interferometry. To verify vertical displacement maps obtained from radar interferometry data using GNSS data from observations at permanent stations.

Input data. Daily 30-second RINEX-files used in the study and time series of daily GNSS solutions of BYCH, GORD, CRNT stations for the period from 16.12.2019 to 01.01.2020 were obtained on the basis of processing of radar interferometry data. The daily solutions were obtained using Bernese GNSS Software [Dach et al., 2015] according to the recommendations of the International

Earth Rotation Service and reference systems IERS Conventions (2010) [Petit, Luzum, 2010]. Table 1 presentsthe time series of vertical displacement of GNSS stations for the period from 16.12.2019 to 01.01.2020 relative to the epoch of their introduction into service. There are no solutions for 17.12.2019 for BYCH and CRNT due to technical reasons.

Radar images obtained by the Sentinel-1A satellite mission provided by the Copernicus program were used to develop maps of the vertical displacements of the Earth's surface.

The Copernicus Program is an environmental monitoring program coordinated by the European Commission and the European Space Agency (ESA). ESA is currently developing seven Sentinel missions (Sentinel 1, 2, 3, 4, 5P, 5, 6). Sentinel missions receive radar and hyper-spectral images for analysis and monitoring of land, ocean and atmosphere. The program's goal is to provide global, continuous, autonomous, high-quality and wide-ranging monitoring of the Earth. In addition, the main concept of the program is to provide a free access to remote sensing data of various missions through the portal Copernicus Open Access Hub [Kumar, 2021].

The Open Access Hub service automatically selects available radar images from storage while setting the spatial and temporal boundaries of the study area.

Radar satellite images from the Sentinel-1A spacecraft were downloaded from the Open Access Hub portal for studying vertical displacements of the Earth's surface in the study area. Data type — SLC (Single Look Complex) with vertical polarization. Acquisition mode is broadband interferometry IW (Interferometric Wide Swath).

The differential interferogram is made ac-

Table 1. Time series of vertical displacement of GNSS stations during 16.12.2019—01.01.2020

Day number from the beginning of the year	Date	Vertical displacement of the GNSS station relative to the epoch of introduction into service, m		
		BYCH	CRNT	GORD
350	16.12.19	13.0	7.5	0.0
351	17.12.19	—	—	0.9
352	18.12.19	14.6	9.5	0.8
353	19.12.19	13.8	6.2	8.9
354	20.12.19	17.1	10.5	10.4
355	21.12.19	18.0	11.2	13.1
356	22.12.19	19.0	10.5	17.0
357	23.12.19	18.3	11.2	11.2
358	24.12.19	15.0	9.2	14.5
359	25.12.19	14.3	7.8	11.8
360	26.12.19	10.4	3.8	9.7
361	27.12.19	3.0	–4.2	1.5
362	28.12.19	2.7	–3.8	–0.3
363	29.12.19	–3.6	–7.8	–2.2
364	30.12.19	–1.1	–5.9	–2.2
365	31.12.19	0.1	0.7	1.8
1	01.01.20	0.0	–5.0	–1.5

Table 2. Spatio-temporal distribution of displacements of the Earth's surface under the NTAL influence and radar data

Name of GNSS station	Periods of the earth surface displacement	The period between acquisitions	The name of the downloaded file
BYCH (Buchach)	22.12.2019 (356) — 29.12.2019 (363)	18.12.2019 —30.12.2019	S1A_IW_SLC__1SDV_20191218T160209_ 20191218T160237_030405_037AC0_42E7 S1A_IW_SLC__1SDV_20191230T160208_ 20191230T160236_030580_0380C4_D374
GORD (Horodok)	17.12.2019 (351) — 22.12.2019 (356) 22.12.2019 (356) — 28.12.2019 (362)	18.12.2019 —30.12.2019	S1A_IW_SLC__1SDV_20191218T160209_ 20191218T160237_030405_037AC0_42E7 S1A_IW_SLC__1SDV_20191230T160208_ 20191230T160236_030580_0380C4_D374
		22.12.2019 —03.01.2020	S1A_IW_SLC__1SDV_20191222T042039_ 20191222T042106_030456_037C7F_77B9 S1A_IW_SLC__1SDV_20200103T042038_ 20200103T042105_030631_038284_AFE4
CRNT (Chernivtsi)	23.12.2019 (357) — 29.12.2019 (363)	18.12.2019 —30.01.2020	S1A_IW_SLC__1SDV_20191218T160144_ 20191218T160211_030405_037AC0_4BC3 S1A_IW_SLC__1SDV_20191230T160144_ 20191230T160211_030580_0380C4_AC4B

cording to the data of two acquisitionscarried out with intervals of 12 days apart. The selection of pairs of radar images was performed in such a way that the maximum vertical displacements of the Earth's surface (according to the time series of GNSS) occur in the period between the acquisitions. The information about downloaded files and sensing periods are presented in the Table 2.

Data of Sentinel-1 radar images were processed with specialized SNAP software.

Data processing algorithm. Processing of interferometric Sentinel-1A images and developing a vertical displacements map consist of a series of operations [Small, Schubert, 2019], here structured as follows:

Co-registration and interferogram formation. The satellites' orbits were corrected (Apply Orbit File) based on high-precision orbital data. The operation is performed separately for each image. Co-registration and back geocoding were performed using the ACE30 digital elevation model. A product containing data on phase variations was produced by Interferogram Formation. After the gaps (bursts) were removed and a solid image was produced (Deburst), we obtained a continuous interferogram of the selected area.

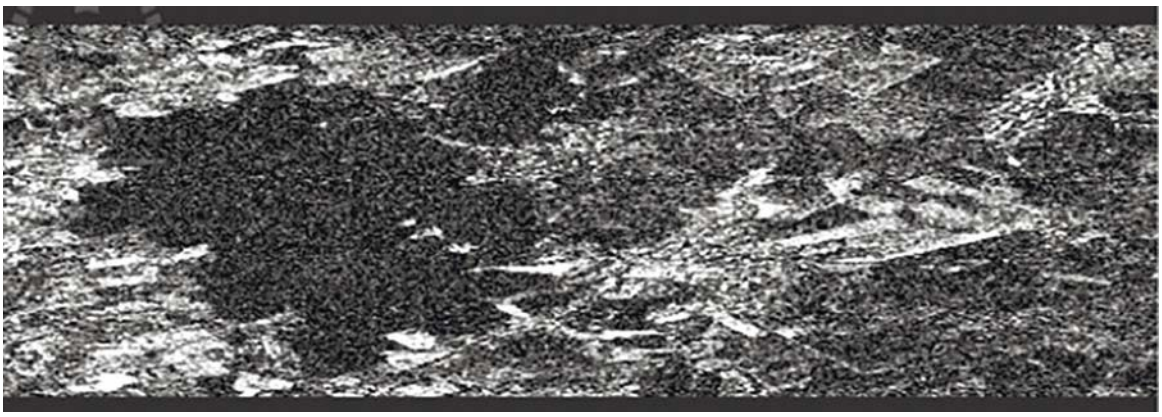

Fig. 3. Coherence map: white areas of high coherence; dark areas of low coherence.

The resulting file contains a coherence map (Fig. 3) besides the generated interferogram. Coherence is calculated as a separate swath and shows how similar each pixel is between master and slave images [Braun, 2021]. The coherence value varies from 0 (no image coherence) to 1 (maximum coherence value).

Creating a differential interferogram and phase filtering. The interferogram formed at the previous step contains data of vertical displacements and a relief. By filtering out the relief component, we obtain a differential interferogram. It represents only the movement of the Earth's surface.

The interferometric step can be corrupted by noise due to: temporal decorrelation; geometric decorrelation; volume scattering; processing errors. In order to improve the quality of the interferogram analysis in the following steps, the signal-to-noise ratio was increased by applying Goldstein Phase Filtering.

With noise was removed, the visibility of interferometric bands was significantly improved (Fig. 4) [Goldstein, Werner, 1998].

At the end of the second stage, the generated results were exported from the SNAP (SNAPHU export) for two-dimensional phase deployment according to the SNAPHU algorithm (Statistical-cost, Network-flow Algorithm for Phase Unwrapping).

Phase Unwrapping using SNAPHU. The SNAPHU algorithm solves the problem of ambiguity of the phase signal of the interferogram. The meaning of the ambiguity is that the absolute phase is wrapped into the interval $[\pi; +\pi]$, while the real value of the phase reaches tens of radians.

Fig. 5 shows the interferogram before and after phase unwrapping. As a result of unwrapping, the phase range changed from [–3.141; +3.141] (Fig. 5, *a*) to [–9.715; +20.498] (Fig. 5, *b*).

Development of vertical displacements map. The unwrapped phase of the differential interferogram is a continuous raster, but does not contain metric data. Phase units measured in radians are converted into metric units, and the vertical displacement map is projected onto the WGS84 coordinate system. Data with coherence level >0.4 were used for further processing. The data was exported as a KMZ file for a preview via Google Earth.

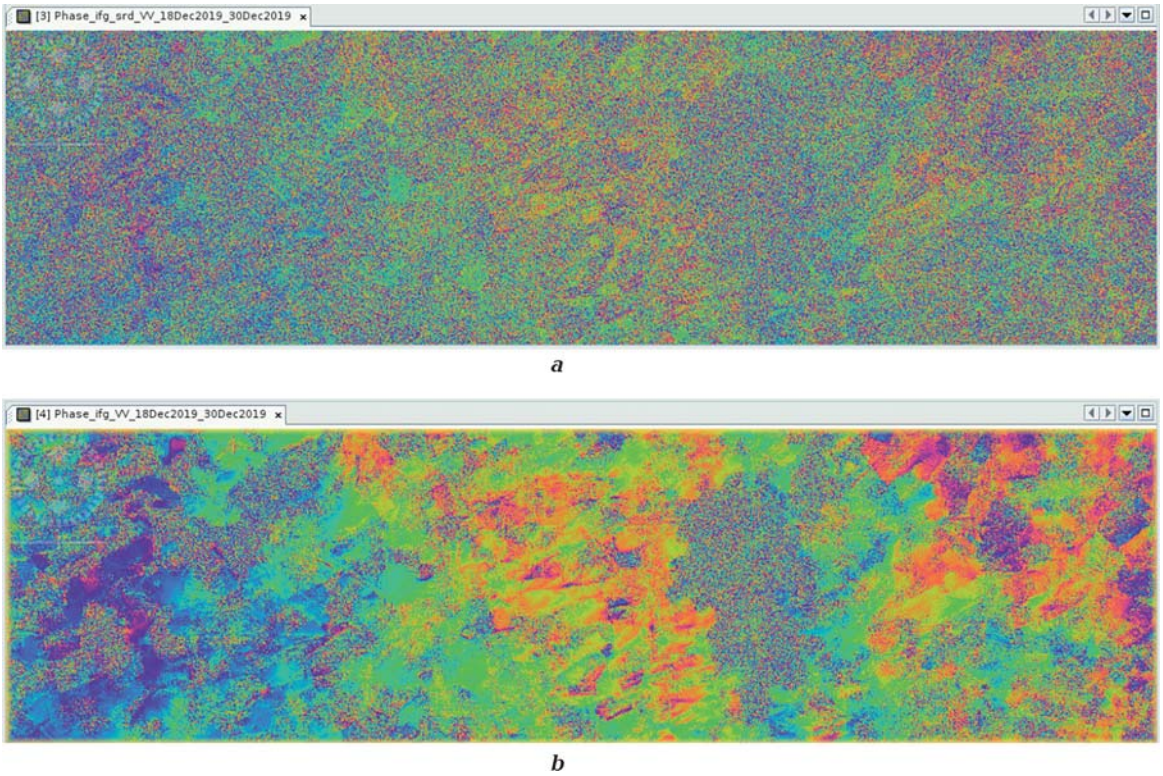

Fig. 4. Differential interferogram before (*a*) and after filtering (*b*) Goldstein Phase Filtering.

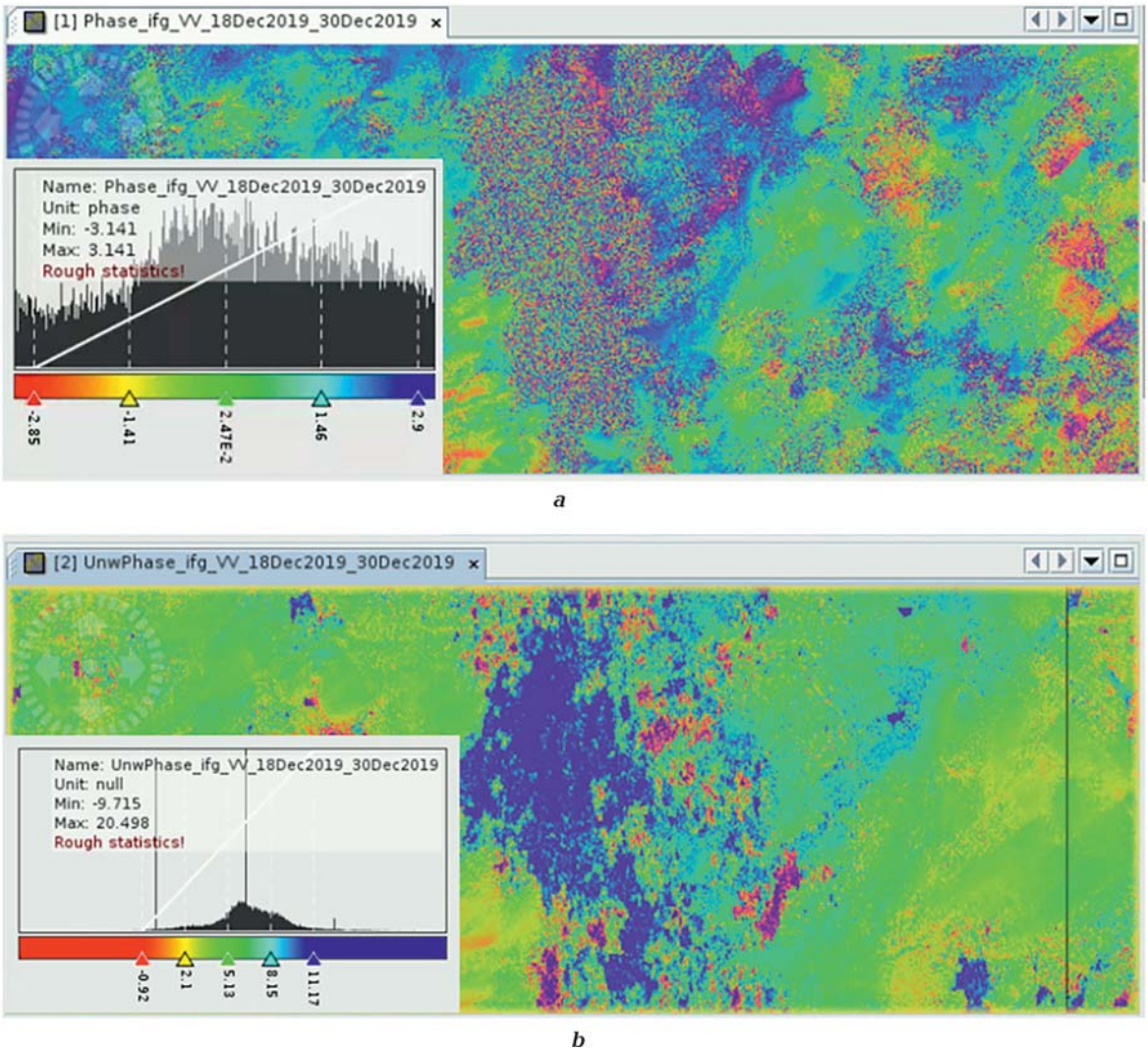

Fig. 5. Differential interferogram before (*a*) after phase unwrapping (*b*).

Results. According to the algorithm described above, pairs of radar images were processed (see Table 1) for three selected areas around the cities: Buchach, Horodok, and Chernivtsi, where GNSS stations are located. Let us analyze the results for each area.

Buchach. GNSS station in Buchach has recorded vertical subsidence by 22 mm, which began on 22.12.19 and ended on 29.12.19. Fig. 6, *a*, *b* show the time series of changes in the altitude position of the permanent GNSS station BYCH with the indicated moments of satellite images (master/slave image) and the forecast model of displacements of the earth's surface due to NTAL (Fig. 6, *c*).As seen from Fig. 6, *b* and 6, *c*, the forecast model is almost identical to the time series data of the GNSS station BYCH. A synchronous uplift of the GNSS station and then a rapid subsidence were established by both methods. According to the GNSS data, the uplift was slower than according to the forecast model. However, the maximum subsidence according to the forecast model reaches 24 mm, which almost coincides with the GNSS data.

A vertical displacement map of Buchachand the surrounding territory was made on the basis of radar images (Fig. 7). InSAR-acquisition was performed on 18.12.19 and 30.12.19.

On the map of vertical displacements (see Fig. 7), results of subsidence of the Earth's

surface were obtained, which are mainly in the range of 20—30 mm, which almost coincides with the GNSS measurements and the forecast model of displacements of the earth's surface due to NTAL. At some points, the maximum vertical displacement was 50 mm. It might be caused by the heterogeneous geological structure of the territories and different characteristics of soils and rocks. It can also be a result of low coherence of the images in these areas and accordingly, these results are much less credible. The obtained point results directly near the GNSS station BYCH record a subsidence of about 28 mm. The difference in the values of the vertical displacements obtained from the time series of GNSS observations and from differential interferogram is 6 mm.

It should be noted that a large part of the study area is covered with forests, which do not allow acquiring information about the movement of the territory.

Horodok. Time series analysis of the vertical displacements of the GNSS station GORD (Fig. 8, *a*, *b*) shows a rapid uplift by 16 mm from 18.12. to 22.12.2019 and its subsidence

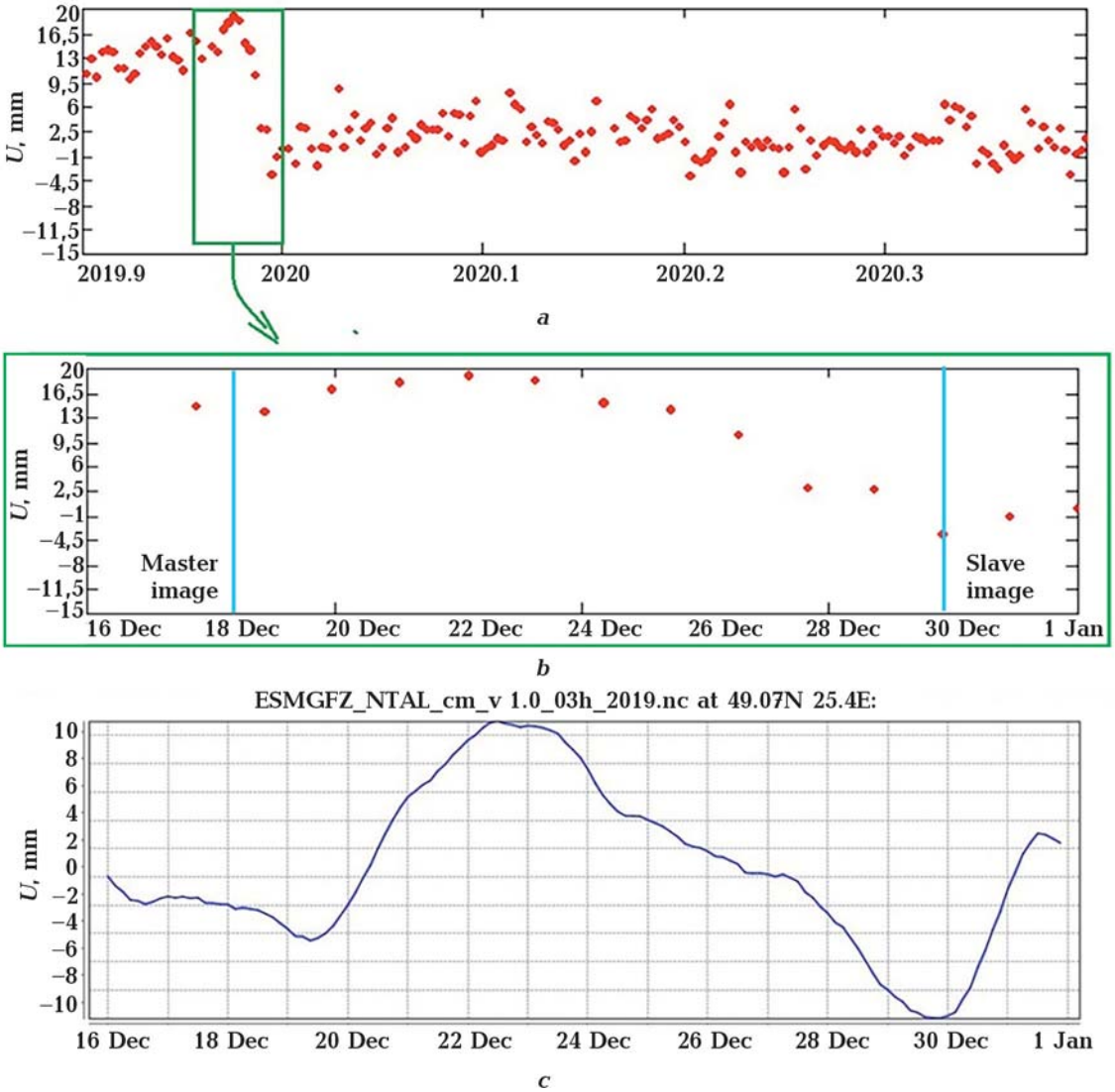

Fig. 6. Time series of permanent GNSS station BYCH altitude changes: *a* — for the period from November 24, 2019 to January 1, 2020; *b* — for the period from December 16, 2019 to January 1, 2020; and the moments of satellite acquisition; *c* — GFZ calculated for non-tidal atmospheric load based on atmospheric surface pressure [ESMGFZ].

from 22.12. to 12.29.2019 by 20 mm. The model of NTAL-induced surface displacements (Fig. 8, *c*), predicts the same (an uplift of 17 mm and a subsidence of 20 mm). That is, the GNSS measurement data and the forecast model herecoincide. Fig. 8, *b* shows the moments of satellite acquisitions (master/slave image).

According to the results of processing of the repeated satellite images in Horodok area, maps of vertical displacements for two time periods were developed: before and after the completion of vertical displacements of the territory; from the moment of maximum rising of GNSS station to its maximum subsidence and stabilization of altitude position.

Since the process of vertical displacements was in the interval between acquisitions (18—30.12.19), there no significant vertical displacements for Horodok are found on the map (Fig. 9, *a*). The measured values of vertical displacements for particular points are in the range from –5 mm to +5 mm, which is close to the results of GNSS measurements (total subsidence 5 mm) and data for calculating the forecast model of displacements of the earth surface due to NTAL (subsidence 6 mm). The point results directly near the GNSS station GORD record an uplift of 5 mm.

According to the second pair of images, which covers the period from 22.12.19 to 03.01.20, a vertical displacements map was made (Fig. 9, *b*), which shows subsidence in the vast majority of the territory (range of displacements from –36 mm to +1 mm). Similar displacements were recorded during this period by the GNSS station GORD (subsidence 18 mm) and according to the forecast model of displacement of the earth surface due to NTAL (subsidence 10 mm). The obtained point results directly near the GNSS station GORD record a subsidence by about 8 mm. The difference in the vertical displacements obtained from the time series of GNSS observations and from differential interferogram is 10 mm.

Chernivtsi. According to the GNSS measurements in Chernivtsi at the CRNT station, a subsidence of 20 mm was recorded, which began on December 23, and ended on December 29, 2019 (Fig. 10, *a*, *b*). According to the forecast model data of the Earth's surface displacement due to NTAL, there was a synchronous subsidence of this area by 19 mm

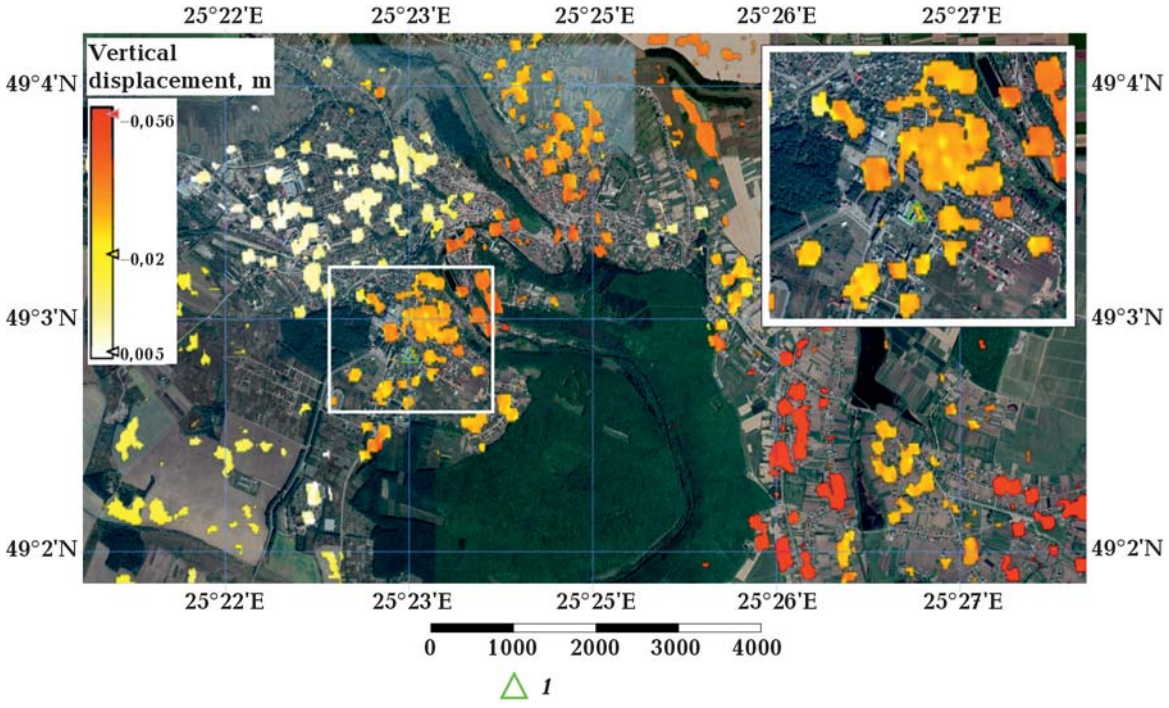

Fig. 7. Vertical displacements map of Buchach (acquisitions 18.12.2019—30.12.2019): *1* — GNSS station.

(Fig. 10, *c*) during this period. Fig. 10, *b* presents the moments of satellite acquisitions (master/slave image) of this territory.

A vertical displacements map was made for this territory (Fig. 11) for the observation period of 18.12.19—30.12.19.

During thisperiod the average subsidence of 20—25 mm was recorded in the majority of the territory (see Fig. 11). The surrounding area reacts differently to the effects of non-tidal atmospheric load. In some points the displacement reaches -60 mm. The obtained point results directly near the GNSS station CRNT record a subsidence of about 22 mm.

During the same period, according to the GNSS station there was a subsidence of 17 mm and according to the forecast model data, there was a subsidence of this area by 8 mm. The general trend is confirmed by all three methods.

The variation in vertical displacements obtained from the time series of GNSS observations and from differential interferogram is 5 mm.

Conclusions. 1. The application of radar

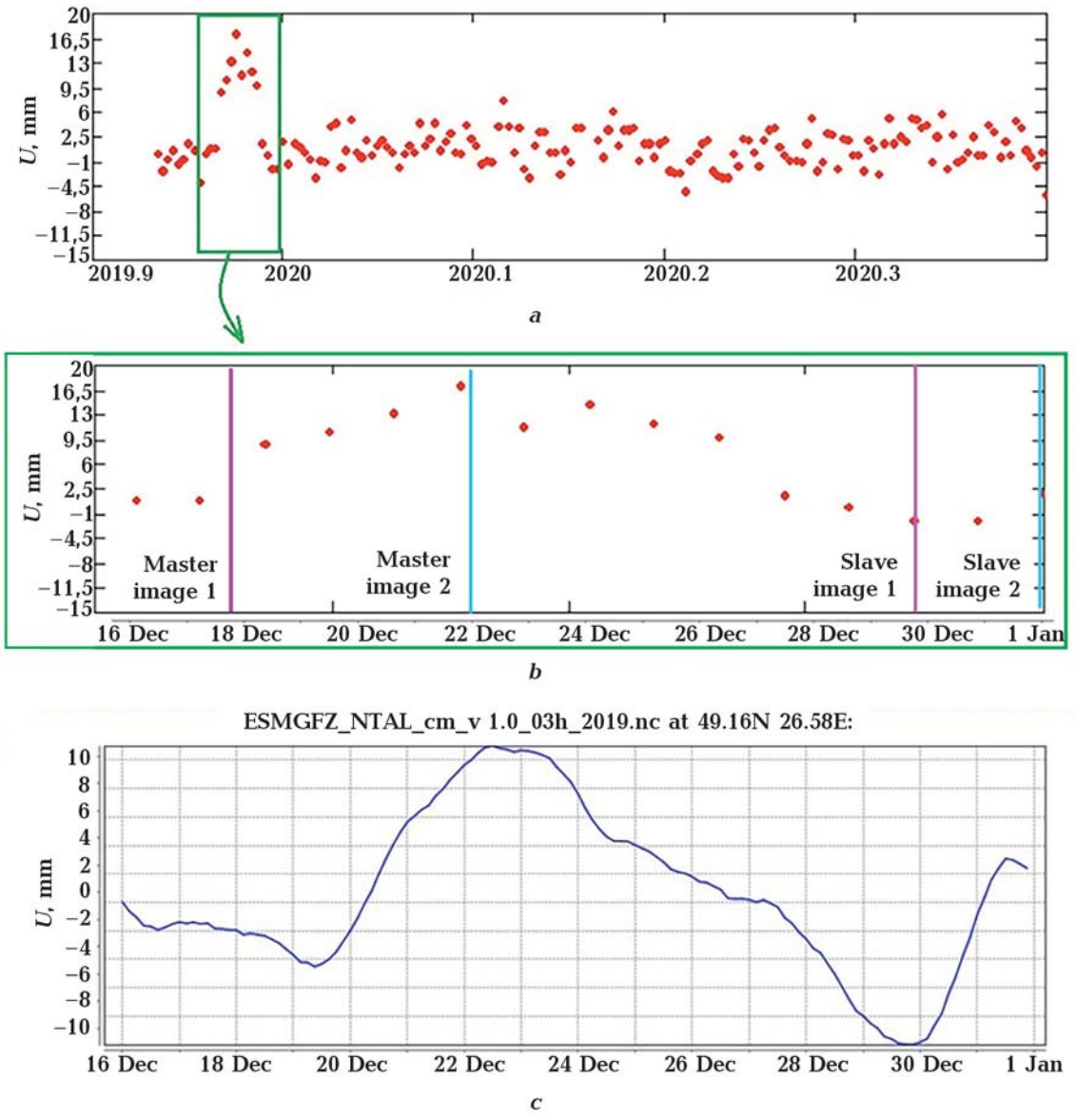

Fig. 8. Time series of permanent GNSS station GORD altitude changes: *a* — for the period of November 24, 2019 to January 1, 2020; *b* — for the period of December 16, 2019 to January 1, 2020 (and the moments of satellite acquisitions); *c* — GFZ calculated for non-tidal atmospheric load based on atmospheric surface pressure [ESMGFZ].

interferometric images of Sentinel-1 mission (the shortest time between acquisitions being 12 days) for detecting short-period displacements of the earth's surface under the influ-

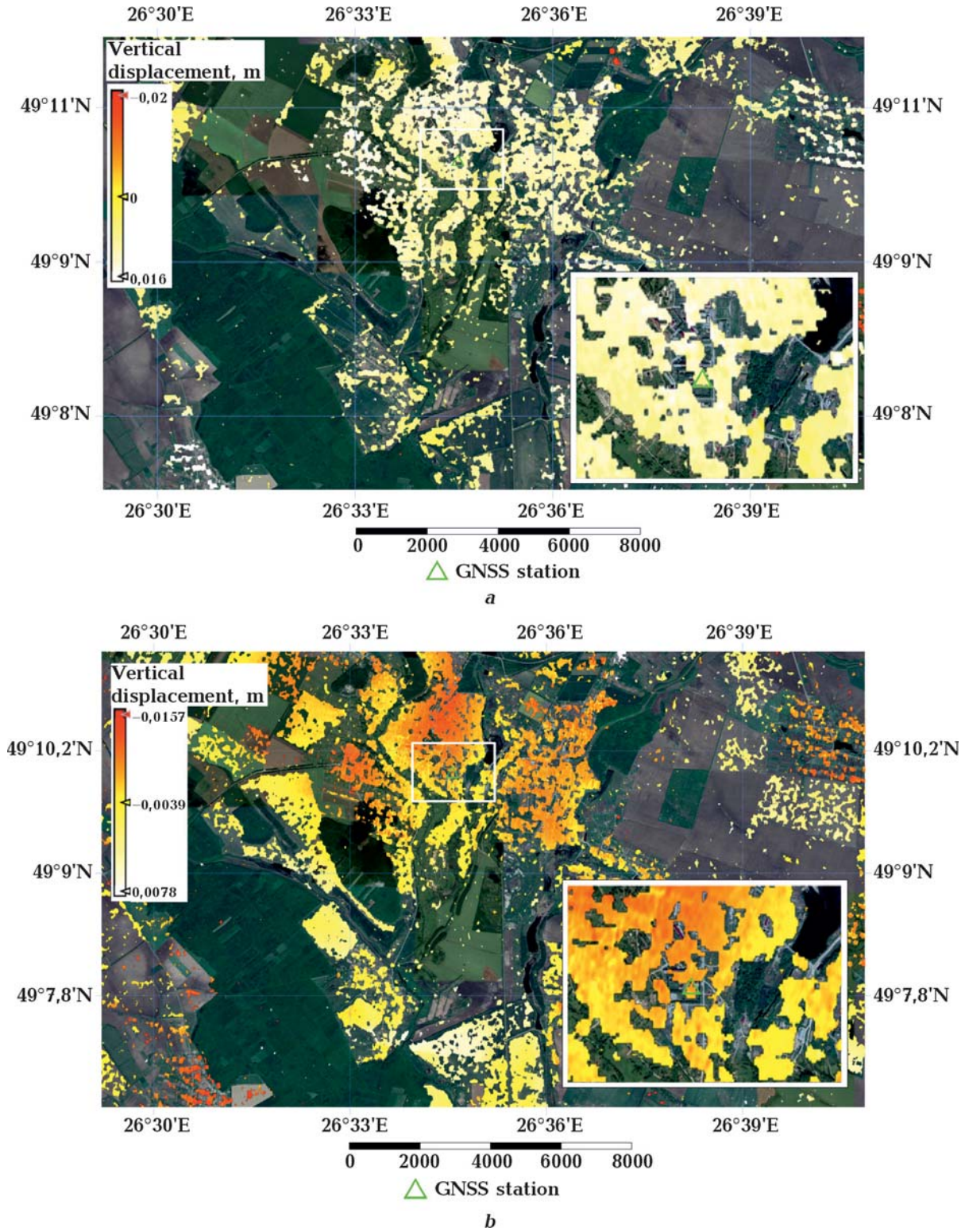

Fig. 9. Vertical displacements map of Horodok: *a* — acquisitions 18.12.2019—30.12.2019; *b* — acquisitions 22.12.19—03.01.20.

ence of non-tidal atmospheric load (NTAL) was validated.

2. The vertical displacements obtained on the basis of differential interferograms are determined with millimeter accuracy. The data confirm the results of displacements obtained during these periods by GNSS stations. The differences in the vertical displacements obtained from the time series of GNSS observations and from differential interferograms do not exceed 1 cm and they are predetermined by errors of radar interferometric acquisitions and GNSS measurements.

3. Predictive parameters of vertical displacements affected by NTAL are created on the basis of atmospheric data of the European center of medium-term weather forecast. These calculations use the average density of the Earth's crust and do not take into account the peculiarities of the geological structure of the region. Obviously, therefore, the vertical displacements may have an abnormal spatial distribution in the study area, as confirmed by the results of radar image processing.

4. Studies of NTAL impact according to GNSS measurements yield vertical displace-

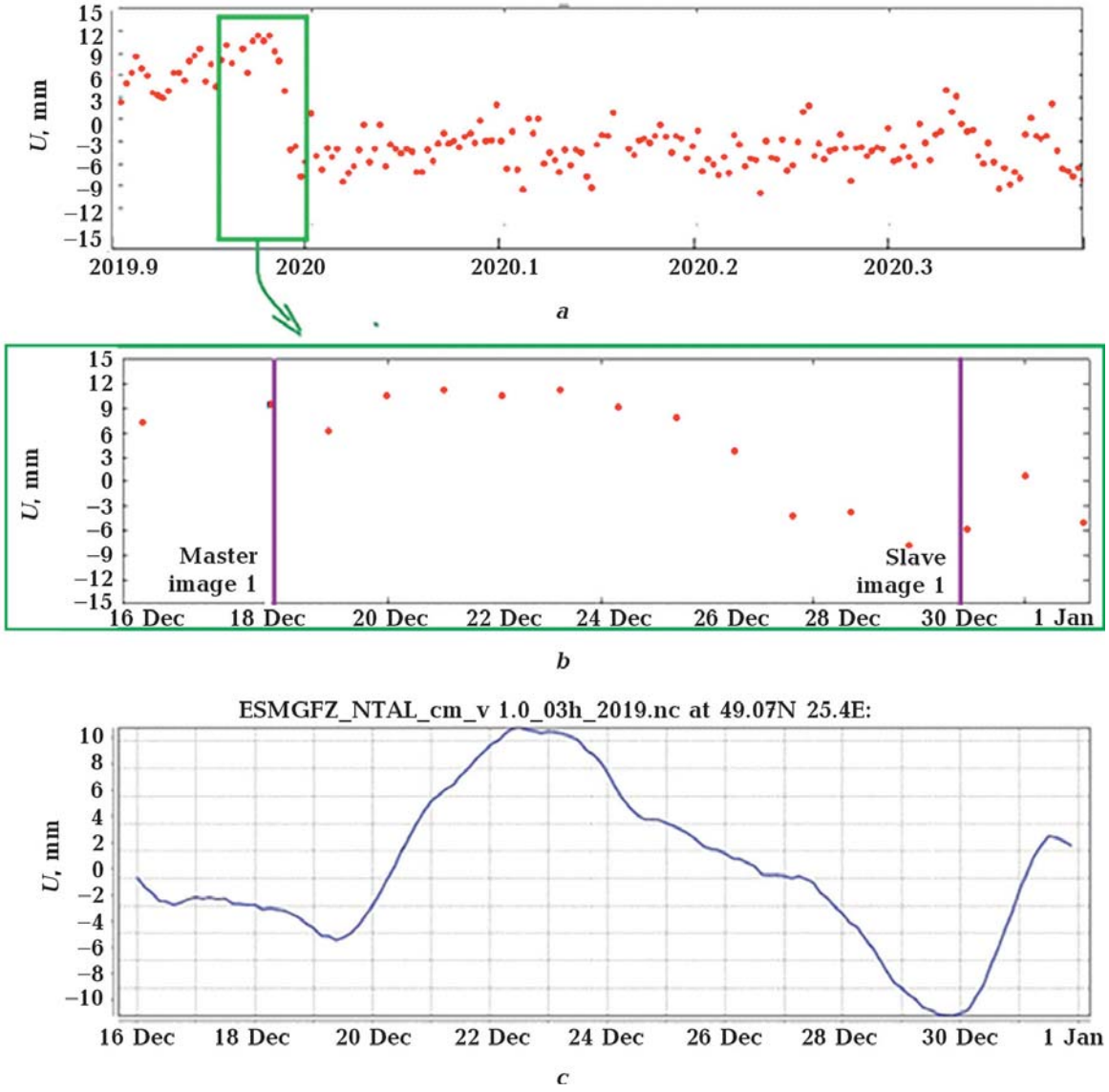

Fig. 10. Time series of permanent GNSS station CRNT altitude changes: *a* — for the period from November 24, 2019 to January 1, 2020; *b* — for the period from December 16, 2019 to January 1, 2020 and the moments of satellite acquisitions; *c* — GFZ calculated for non-tidal atmospheric load based on atmospheric surface pressure [ESMGFZ].

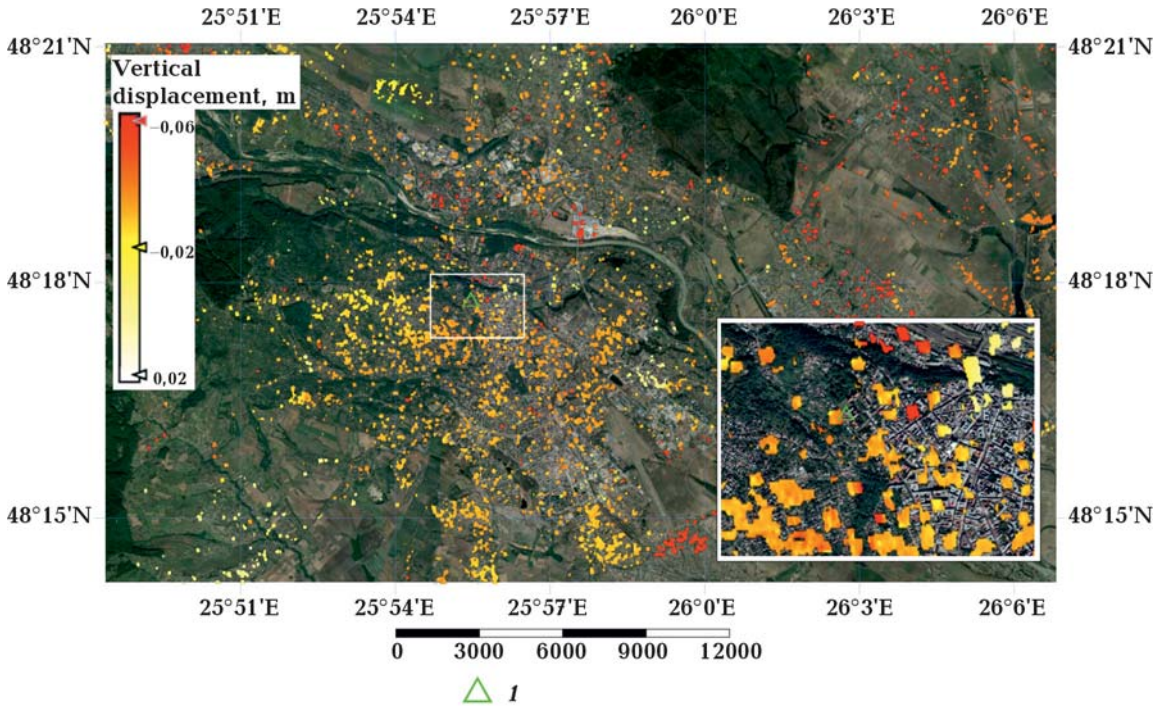

Fig. 11. Vertical displacements map of Chernivtsi (acquisitions 18.12.2019—30.12.2019): *1* — GNSS Station.

ments only for the stations' locations. By using radar interferometry, we obtain a spatial distribution of displacements for large areas within the satellite image.

5. Development of vertical displacements map of the Earth's surface predetermined by NTAL has both scientific and practical importance for the study of its impact. The practical significance of the obtained results is to increase the accuracy of terrestrial geodetic measurements processing, in particular high-precision levelling. During the levelling process, which takes a while, the benchmarks can change their vertical position under the influence of atmospheric load (NTAL). Our findings help to correct the levelling results for short-period displacement caused by the influence of NTAL.

6. It is possible to differentiate the territory into areas that react differently to the impact of NTAL on the basis of long-term monitoring by InSAR methods.

Acknowledgement. We are grateful for the team of the Research and User Support, that has worked within the Copernicus project toprovide access to the online platform and virtual computing resources. The service granted access not only to the Copernicus data and software tools, but also to a wide selection of training materials.

References

Amitrano, D., Guida, R., Di Martino, G., & Iodice, A. (2019). Glacier Monitoring Using Frequency Domain Offset Tracking Applied to Sentinel-1 Images: A Product Performance Comparison. Remote Sensing, *11*(11), 1322. https://doi.org/ 10.3390/rs11111322.

Braun, A. (2021). Retrieval of digital elevation models from Sentinel-1 radar data — open applications, techniques, and limitations. *Open Geosciences, 13*(1), 532—569. https://doi.org/10.1515/geo-2020-0246.

Brusak, I., & Tretyak, K. (2020). About the phenomenon of subsidence in continental Europe in December 2019 based on the GNSS stations data. *International Conference of Young Professionals «GeoTerrace-2020»* (pp. 1—5). https://doi.org/10.3997/2214-4609.20205717.

Crosetto, M., Monserrat, O., Cuevas-González, M., Devanthéry, N., & Crippa, B. (2016). Persistent Scatterer Interferometry: A review. *Journal of Photogrammetry and Remote Sensing, 115*, 78—89. https://doi.org/10.1016/j.isprsjprs.2015.10.011.

Dach, R., Lutz, S., Walser, P., & Fridez, P. (Eds.). (2015). *Bernese GNSS software, Version 5.2*. https://doi.org/10.7892/boris.72297.

Dorosh, L., & Gera, O. (2020). Satellite monitoring of the mining lease areas using radar interferometry data. *Proc. of the XXV International Scientific-Technical Conference «Geoforum-2020», April 1—3, 2020* (pp. 31—35).

ESMGFZ Product Repository; Earth System Modelling at GFZ. Retrieved from http://esmdata.gfz-potsdam.de.

Gobron, K., Rebischung, P., Van Camp, M., Demoulin, A., & Viron, O. (2021). Influence of aperiodic non-tidal atmospheric and oceanic loading deformations on the stochastic properties of global GNSS vertical land motion time series. *Journal of Geophysical Research: Solid Earth, 126*(9). https://doi.org/10.1029/2021JB022370.

Goldstein, R., & Werner, C. (1998). Radar interferogram filtering for geophysical applications. *Geophysical Research Letters, 25*(21), 4035—4038. https://doi.org/10.1029/1998GL900033.

Gómez, D., Salvador, P., Sanz, J., Urbazaev, M., & Casanova, J.L. (2020). Analyzing ice dynamics using Sentinel-1 data at the Solheimajoküll Glacier, Iceland. *GIScience & Remote Sensing, 57*(6), 813—829. https://doi.org/10.1080/15481603.2020.1814031.

Jungclaus, J.H., Fischer, N., Haak, H., Lohmann, K., Marotzke, J., Matei, D., Mikolajewicz, U., Notz, D., & von Storch, J.S. (2013). Characteristics of the ocean simulations in MPIOM, the ocean component of the MPI-Earth system model. *Journal of Advances in ModelingEarth Systems, 5*(2), 422—446. https://doi.org/10.1002/jame.20023.

Klos, A., Dobslaw, H., Dill, R., & Bogusz, J. (2021). Identifying the sensitivity of GPS to non-tidal loadings at various time resolutions: examining vertical displacements from continental Eurasia. *GPS Solutions, 25*, 89. https://doi.org/10.1007/s10291-021-01135-w.

Kumar, D. (2021). Urban objects detection from C-band synthetic aperture radar (SAR) satellite images through simulating filter properties. *Scientific Reports, 11*, 6241. https://doi.org/10.1038/s41598-021-85121-9.

Li, S., Xu, W., & Li, Z. (2022). Review of the SBAS InSAR Time-series algorithms, applications, and challenges. *Geodesy and Geodynamics, 13*(2), 114—126. https://doi.org/10.1016/j.geog.2021.09.007.

Lu, Z., Dzurisin, D., Biggs, J., Wicks, C.Jr., & McNutt, S. (2010). Ground surface deformation patterns, magma supply, and magma storage at Okmok volcano, Alaska, from InSAR analysis: 1. Intereruption deformation, 1997—2008. *Journal of Geophysical Research, 115*, B00B02. https://doi.org/10.1029/2009JB006969.

Mémin, A., Boy, J.P., & Santamaría-Gómez, A. (2020). Correcting GPS measurements for non-tidal loading. *GPS Solutions, 24*, 45. https://doi.org/10. 1007/s10291-020-0959-3.

Petit, G., & Luzum, B. (Eds.). (2010). *IERS Conventions (IERS Technical Note; 36)*. Frankfurt am Main: Verlag des Bundesamts für Kartographie und Geodäsie.

Petrov, L. (2015). The international mass loading service. In *REFAG 2014* (pp. 79—83). Springer, Cham. https://doi.org/10.1007/1345_2015_218.

Schaefer, L.N., Lu, Z., & Oommen, T. (2015). Dramatic volcanic instability revealed by InSAR. Geology, *43*(8), 743—746. https://doi.org/10.1130/G36678.1.

Sheng, Y., Wang, Y., Ge, L., & Rizos, C. (2009). Differential radar interferometry and its application in monitoring underground coal mining-induced subsidence. *Environmental Science*. Retrieved from https://www.isprs.org/proceedings/XXXVIII/7-C4/227_GSEM2009.pdf.

Small, D., & Schubert, A. (2019). *Guide to Sentinel-1 Geocoding*. Retrieved from https://sentinel.esa.int/ documents/247904/1653442/Guide-to-Sentinel-1-Geocoding.pdf.

Stankevych, S.A., Svidenyuk, M.O., & Dudar, T.V. (2019). Radar interferometry time series analysis for land surface displacement detection within the uranium mining area in Ukraine. *Ecological safety, 2*(28), 18—23. http://doi.org/10.30929/2073-5057.2019.2.18-23 (in Ukrainian).

Tretyak, K., Brusak, I., Bubniak, I., & Zablotskyi, F.

(2021). Impact of non-tidal atmospheric loading on civil engineering structures. *Geodynamics, 2*(31), 16—28. https://doi.org/10.23939/jgd2021.02.016

Tzouvaras, M., Danezis, C., & Hadjimitsis, D.G. (2020). Differential SAR Interferometry Using Sentinel-1 Imagery-Limitations in Monitoring Fast Moving Landslides: The Case Study of Cyprus. *Geosciences, 10*(6), 236. https://doi.org/10.3390/geosciences10060236.

Uglytskykh, Ye., Vyzhva, S., & Ivanik, O. (2020). Vertical displacement monitoring of Zakarpattya region territory based on radar interferometry data. *Visnyk of Taras Shevchenko National University of Kyiv. Geology,* (4), 94—99. http://doi.org/10.17721/1728-2713.91.13 (in Ukrainian).

VMF Data Server; editing status 2020-12-14; re3data.org — Registry of Research Data Repositories. http://doi.org/10.17616/R3RD2H.

Застосування радарних інтерферометричних знімків Sentinel-1 для моніторингу вертикальних зміщень земної поверхні, викликаних неприпливним атмосферним навантаженням

К.Р. Третяк*[1], *Д.В. Кухтар*[2], *2003

[1]Національний університет
«Львівська політехніка», Львів, Україна
[2]Івано-Франківський національний технічний
університет нафти і газу, Івано-Франківськ, Україна

Проаналізовано вертикальні рухи земної поверхні, зумовлені впливом неприпливного атмосферного навантаження NTAL, за допомогою даних супутникової радарної інтерферометрії. Встановлено чіткий зв'язок між даними карт вертикальних зміщень, отриманих за результатами радарної інтерферометрії, та висотними часовими рядами перманентних ГНСС станцій. Об'єкт дослідження — територія довкола ГНСС станцій BYCH (м. Бучач), GORD (м. Городок), CRNT (м. Чернівці). Вхідними даними були чотири пари радарних інтерферометричних знімків зазначені територій. Радарні супутникові знімки отримано з космічного апарату Sentinel-1A. Тип даних — SLC (Single Look Complex) з вертикальною поляризацією. Режим знімання — широкосмугова інтерферометрія IW (Interferometric Wide Swath). Дані опрацьовано проводилось за допомогою програмного забезпечення SNAP (Sentinel Application Platform). У результаті опрацювання радарних інтерферометричних знімків отримано карти вертикальних зміщень указаних територій, де відбувалось зміщення земної поверхні, зумовлене впливом неприпливного атмосферного навантаження. Значення, отримані на основі карт вертикальних зміщень, мають високу збіжність із результатами часових рядів зміни висотного положення перманентних ГНСС станцій. Результати, отримані в статті, мають як наукове, так і практичне значення для вивчення впливу неприпливного атмосферного навантаження на значних територіях — підвищення точності опрацювання наземних геодезичних вимірів, зокрема високоточного нівелювання. За даними досліджень можна вносити поправки у результати нівелювання за короткоперіодичні зміщення, викликані впливом неприпливного атмосферного навантаження NTAL.

Ключові слова: часові ГНСС ряди, вертикальні зміщення, неприпливне атмосферне навантаження, радарна інтерферометрія, Sentinel-1.